

Received December 05, 2020; reviewed; accepted January 11, 2021

Insight into the effect of galvanic interactions between sulfide minerals on the floatability and surface characteristics of pyrite

Bo Yang^{1,2,4}, Xiong Tong^{3,4}, Xian Xie^{3,4}, Lingyun Huang^{3,4}

¹ Faculty of Environmental Science and Engineering, Kunming University of Science and Technology, Kunming 650093, China

² Kunming University, Kunming 650214, China

³ Faculty of Land Resource Engineering, Kunming University of Science and Technology, Kunming 650093, China

⁴ State Key Laboratory of Complex Nonferrous Metal Resources Clean Utilization, Kunming University of Science and Technology, Kunming 650093, China

Corresponding authors: xianxie2008@kmust.edu.cn (Xian Xie), yangbo2018kmu@126.com (Bo Yang)

Abstract: Complex sulfide ores are usually found as a mixture of various sulfide and gangue minerals, and froth flotation is the predominant method for the selective separation of sulfide minerals. Adherence and contact between sulfide minerals are inevitable during froth flotation, and galvanic interactions between sulfide minerals will occur because of differences in rest potentials. However, the effect of these galvanic interactions on the selective flotation of sulfide minerals have been rarely studied. In this work, the effect of the galvanic interaction between pyrite and sphalerite on the flotation behavior and surface characteristics of pyrite was investigated by micro-flotation tests, collector adsorption tests, electrochemical techniques and XPS (X-ray photoelectron spectroscopy) surface analysis. The micro-flotation tests indicated that the floatability of pyrite decreased in the pH range of 4.0 to 9.5 and increased under strongly alkaline pH conditions (pH > 10) due to the galvanic interaction. The collector adsorption results demonstrated that the adsorption capacity of the collector on the pyrite surface was significantly reduced because of the galvanic interaction between pyrite and sphalerite. The electrochemical measurements revealed that the decrease in the oxidation current of xanthates to dixanthogen was responsible for the decreasing adsorption capacity of the collector on the pyrite surface. The XPS results indicated that the formation of the $S_2O_3^{2-}$ oxidation product on the pyrite surface decreased at a strongly alkaline pH due to the galvanic interaction. Therefore, pyrite floatability improved at an alkaline pH. These results consistently showed that the galvanic interaction between pyrite and sphalerite had an important influence on the floatability and surface characteristics of pyrite.

Keywords: galvanic interaction, floatability, pyrite, sulfide minerals

1. Introduction

Sulfide minerals such as chalcopyrite, galena, and sphalerite are the most important raw materials in the production of Cu, Pb, and Zn metals. In nature, these sulfide minerals are generally found as a complex mixture that cannot be directly utilized by the metallurgical industry (Urbano et al., 2007; Shen et al., 2019). Therefore, the beneficiation of sulfide minerals is usually necessary prior to metallurgical treatment, and froth flotation is the predominant method for the beneficiation of sulfide minerals in industrial practice (Hu et al., 2020). In froth flotation, sulfide minerals are selectively separated from gangue minerals based on the difference in their surface hydrophobic/hydrophilic characteristics (Reis et al., 2019). Pyrite, as a common sulfide gangue mineral, is widely intergrown with these valuable sulfide minerals. In froth flotation, pyrite has a similar floatability as these sulfide minerals, which leads to difficulty in the selective separation of sulfide minerals from pyrite (Hu et al., 2000; Mu et al., 2016a; Ejtemaei and Nguyen, 2017). To depress pyrite in froth flotation, an abundance of lime is used as the

depressant. Pyrite is strongly hydrophilic under strongly alkaline pH conditions due to the formation of ferric hydroxides and sulfur-oxygen species on its surface (Chandra et al., 2012; Huang et al., 2013; Mu et al., 2016b; Zanin et al., 2019).

However, the selective flotation of sulfide minerals is extremely difficult when ores have a high pyrite content. For example, the Yiliang Pb–Zn ore in Yunnan Province of Southwest China is regarded as the richest Pb–Zn ore in China. The grades of Pb, Zn, and S in this ore is 7.8%, 18.4%, and 34.8%, respectively, and the pyrite content in this ore reaches approximately 51.3%. After flotation beneficiation, the recovery of Zn and Pb in concentrates reaches only 88.3% and 85.7% respectively, although large quantities of collector and depressant are used. In addition, the grades of Pb and Zn in these concentrates are significantly diluted due to the misreporting of pyrite in the concentrates (Yang et al., 2018a). There are two reasons for this problem. One is the competitive adsorption of pyrite for the collector, which can decrease the concentration of xanthates available for galena and sphalerite. This decrease in the xanthate concentration will reduce the floatability of sulfide minerals (Somasundaran and Wang, 2006). The other reason is that the mass production of ferric or ferrous ions in pulp is caused by the surface oxidation of pyrite under alkaline conditions. As a result, the floatability of sulfide minerals decreases due to the adsorption of ferric or ferrous hydroxides on the surface (Owusu et al., 2014; Owusu et al., 2015).

In addition to the above two reasons, some studies have suggested that galvanic interactions between sulfide minerals may be another important factor affecting the selective flotation of sulfide minerals when complex ores have a high pyrite content (Chopard et al., 2017; Aikawa et al., 2020). According to the difference in the rest potential, the common sulfide minerals can be classified in the following increasing order, $ZnS < PbS < CuFeS_2 < FeS_2$, and galvanic interactions will occur when two minerals with different rest potentials come in contact (Liu et al., 2008; Santos et al., 2016). In galvanic interactions, the mineral with a lower rest potential will act as the anode, and surface oxidation will be promoted. The mineral with a higher rest potential will act as the cathode, and surface oxidation will be inhibited (Yang et al., 2018a; Yang et al., 2018b; Lu et al., 2019). The galvanic interaction between sulfide minerals can influence the surface characteristics and flotation behavior of minerals to a certain extent, as illustrated by Fig. 1.

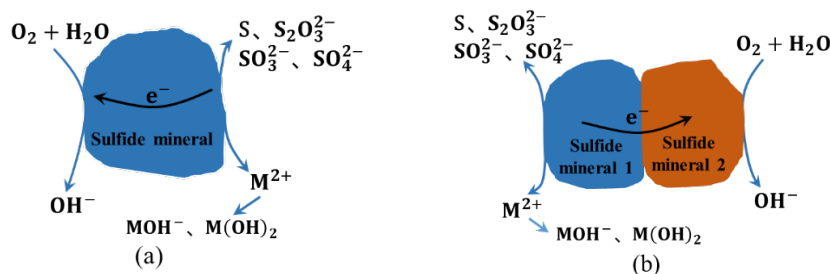


Fig. 1. Schematic diagram showing the galvanic interactions between sulfide minerals: (a) sulfide mineral alone and (b) galvanic interactions

However, many studies on the galvanic interactions between sulfide minerals mainly focus on their effect on the surface characteristics and flotation behavior of valuable minerals (e.g., chalcopyrite, galena, and sphalerite), and less attention is given to the alteration of pyrite after the galvanic interaction. In addition, studying the galvanic interactions between pyrite and other sulfide minerals is meaningful to further understand the difficulty in the selective depression of pyrite during froth flotation. Therefore, the galvanic interaction between pyrite and sphalerite and its effects on the surface characteristics and flotation behavior of pyrite were investigated in this work.

2. Materials and methods

2.1. Materials

The highly mineralized pyrite and sphalerite samples used in this study were obtained from Yiliang Chihong Mining Co., LTD, Yunnan Province, China. After the manual removal of gangue minerals, such as quartz and calcite, the samples were ground in a porcelain ball mill and screened to obtain

minerals with the desired particle size. Then, the samples were stored in polyethylene bags with a N₂ atmosphere to prevent surface oxidation. The chemical compositions of the pyrite and sphalerite samples are listed in Table 1. X-ray diffraction (XRD) results indicated that the samples used in this study were of high purity.

Table 1. Chemical compositions of the sphalerite and pyrite samples

Elements	Zn	Fe	S	Pb	SiO ₂
Pyrite	0.01	52.64	46.24	0.17	0.22
Sphalerite	64.37	0.94	33.71	0.15	0.81

Potassium butyl xanthate (KBX, industrial purity) was used as the collector and further purified by the method described by Song (Song et al., 2000). Methyl isobutylcarbinol (MIBC) was used as the frother. HCl and NaOH (analytical purity) from Tianjin No. 3 Chemical Reagent Factory were used as pH adjusters at concentrations of 0.01 mol/L, and ultrapure water with a resistivity of 18.25 MΩ/cm⁻¹ was used in all of tests.

2.2. Methods

2.2.1. Micro-flotation

Micro-flotation tests were carried out in an XFG flotation machine (Wuhan Exploring Machinery Plant, Hubei, China) with a volume of 40 ml and an impeller speed of 1800 rpm. A 4 g mineral sample with a particle size of -0.074 mm to +0.048 mm was used for each flotation. In the mixed mineral system, a total of 4.0 g mineral mixtures with different proportions of pyrite and sphalerite were used. The sample was first mixed with 40 ml of deionized water, and the pH was adjusted using the 0.01 mol/L HCl and NaOH solutions. After that, the KBX collector and MIBC frother were added and conditioned for 3 min and 1 min, respectively. Finally, the suspension was allowed to float for 3 min. The floating and nonfloating particles were collected, dried and assayed for the recovery calculation. All tests were repeated three times under the same conditions, and the recovery reported in this work is the average.

2.2.2. Collector adsorption tests

The adsorption of the KBX collector on the mineral surface was measured using a UV/Vis spectrophotometer (UV-1800, Shanghai Qinghua Instruments Co., Ltd., Shanghai, China). First, a mineral sample was added to a 100 ml reaction vessel with 40 ml of deionized water, and the pH was adjusted by the HCl and NaOH solutions. Then, the KBX collector was added and conditioned for 3 min. At the end of conditioning, the suspension was quickly transferred to a high-speed centrifuge and separated at 3500 rpm for 3 min. After separation, the supernatant was subjected to the analysis of KBX concentration using a UV/Vis spectrophotometer. At the maximum adsorption peak of 301 nm, the concentration of KBX had a linear relationship with the absorbance of KBX (as shown in Fig. 2), and the concentration of KBX could be calculated from this standard curve.

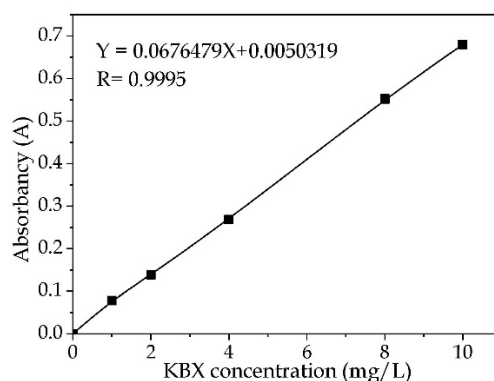


Fig. 2. Absorbance of KBX as a function of the KBX concentration

2.2.3. Voltammetry measurement

Cyclic voltammetry was measured by using an electrochemical workstation (Zahner IM 6, Germany). A traditional three-electrode system consisting of a working electrode, counter electrode (platinum electrode with an area of 1.0 cm²), and reference electrode (Ag/AgCl electrode, 3.0 mol/L KCl) was used. The pyrite electrode was cut from a highly mineralized specimen with a working area of 1.0 cm² as described by Qin (Qin et al., 2015b). Due to the low conductivity of sphalerite, a sphalerite CPE (carbon paste electrode) was used in this study. The electrode was prepared by carefully mixing the -0.038 mm sphalerite particles with graphite powder in an agate mortar, and weight proportions of 80% sphalerite and 20% graphite powder were used. After homogenization, a small amount of liquid paraffin was added and quickly homogenized by using a glass rod. Then, the pastes were quickly compressed by a preforming machine to form a flake with a radius of 0.5 cm. After storage in a N₂ atmosphere for 24 hours, the flake was encapsulated in a glass tube with epoxy resin and connected with copper wire.

To investigate the effect of galvanic interactions on the electrochemical behavior of pyrite, pyrite was electrochemically connected with the sphalerite CPE by using conductive silver adhesives, and only two sides were in contact with the solution (Qin et al., 2015a). The area ratio of the pyrite and sphalerite electrodes exposed to solution was 5:1, and the coupled electrode is illustrated in Fig. 3.

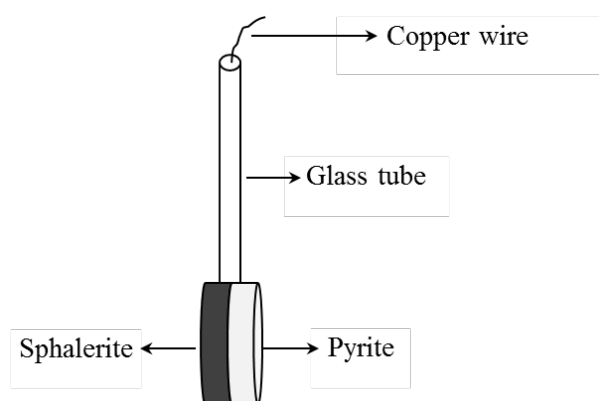


Fig. 3. Schematic diagram showing the coupled sphalerite and pyrite electrode

Cyclic voltammetry tests were carried out at a sweep rate of 10 mV/s, and the solution used in the electrochemical measurements was a buffer solution. After each measurement, a fresh surface was created by polishing the working areas with abrasive paper.

2.2.4. XPS surface analysis

An X-ray photoelectron spectrometer (PHI500, ULVAC-PHI, Kanagawa, Japan) was employed to identify the elements and chemical valence state of the mineral surface. For the mixed mineral system, the sample was prepared by using the following procedure. The 0.5 × 0.5 × 0.2 cm³ pyrite block was wet-polished using abrasive paper to produce a fresh surface. Then, the pyrite was washed with deionized water and immersed quickly in the specified solution in the absence or presence of -0.038 mm sphalerite particles in solution. The surface subjected to XPS analysis was exposed to the solution, and the solution was stirred using a rotary shaker. After stirring, the pyrite block was taken and washed with deionized water at the same pH and dried in a vacuum environment. After that, the XPS measurement was conducted.

3. Results and discussion

3.1. Effect of galvanic interactions on the floatability of pyrite

Flotation tests were carried out to investigate the effect of galvanic interactions between pyrite and sphalerite on the flotation behavior of pyrite when using KBX as the collector. The recovery of pyrite alone and mixed with different proportions of sphalerite as a function of pH are shown Fig. 4.

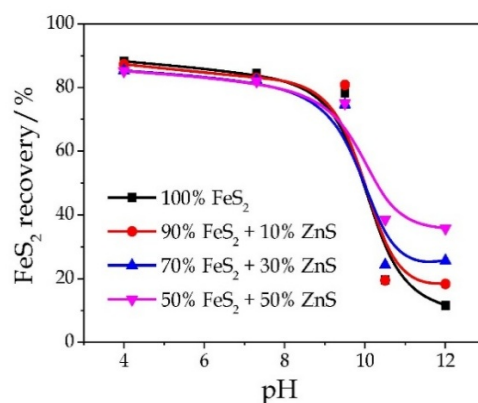


Fig. 4. Flotation behavior of pyrite as a function of pH in the presence and absence of sphalerite (10 mg/L KBX)

It is evident from Fig. 4 that pyrite in the absence of sphalerite exhibited excellent floatability under acidic and weakly alkaline pH conditions ($\text{pH} < 9.5$) and poor floatability under strongly alkaline pH conditions ($\text{pH} > 10.0$), and the recovery decreased with increasing pH. However, compared with pyrite alone, the recovery of pyrite was slightly decreased in acidic and weakly alkaline pH ranges and increased significantly in the strongly alkaline pH range when sphalerite was present in the pulp. In addition, the higher the proportion of sphalerite in the pulp, the higher the flotation recovery for pyrite in the strongly alkaline pH range. It seemed that sphalerite in the pulp depressed the floatability of pyrite under acidic and weakly alkaline pH conditions and increased the floatability of pyrite under strongly alkaline pH conditions.

In the mixed systems of pyrite and sphalerite, there was no competitive adsorption between pyrite and sphalerite for the KBX collector due to the adsorption of KBX on the unactivated sphalerite surface being negligible. The change in the floatability of pyrite could be attributed to the decreasing adsorption of KBX or the increasing surface oxidation of the pyrite surface, which improved the surface hydrophilicity of pyrite. However, many studies have suggested that the surface oxidation of pyrite will be alleviated after galvanic interactions because pyrite usually has the highest rest potential among these common sulfide minerals (Mu et al. 2016b; Moslemi and Gharabaghi 2017; Yang et al. 2018b). Therefore, the decreasing floatability of pyrite was mainly attributed to the decreasing adsorption of KBX on the pyrite surface. Mu and Urbano suggested that the galvanic interaction between sulfide minerals could influence the electrochemical reactivity of mineral surfaces and further influence the floatability of minerals (Urbano et al. 2007; Mu et al. 2018).

3.2 Effects of galvanic interactions on the adsorption of KBX on the pyrite surface

The adsorption of KBX on pyrite surfaces in the absence and presence of sphalerite was conducted to investigate the influence of galvanic interactions on xanthate adsorption, and the results are shown in Fig. 5. In Fig. 5, the y-axis represents the concentration differences of KBX before adsorption (C_0) and after concentration (C_t). The higher the values of $C_0 - C_t$ are, the more KBX adsorbed on the mineral surface.

Fig. 5 shows that the concentration difference ($C_0 - C_t$) of KBX increased with increasing KBX concentration under $\text{pH} = 7.3$ and $\text{pH} = 9.0$ conditions for pyrite alone. The concentration difference was almost unchanged when the KBX concentration was more than 10 mg/L, which indicated that the adsorption of xanthate became saturated at this dosage of KBX. Under the strongly alkaline condition of $\text{pH} = 12$, the adsorption of KBX on the pyrite surface was significantly decreased due to the serious surface oxidation and competitive adsorption of OH^- . In regard to sphalerite alone, the concentration difference of KBX was almost unchanged at all the studied pH conditions because of the poor response of the unactivated sphalerite to the xanthate collector (Zeng et al. 2019). Compared with pyrite alone, however, an obvious decrease in the concentration difference of KBX was observed in the mixed system under $\text{pH} = 7.3$ and $\text{pH} = 9.0$ conditions. Because the adsorption of KBX on the unactivated sphalerite surface was negligible, the decrease in the concentration difference of KBX in the mixed system was mainly attributed to the decreasing adsorption of KBX on the pyrite surface. The results from Fig. 5

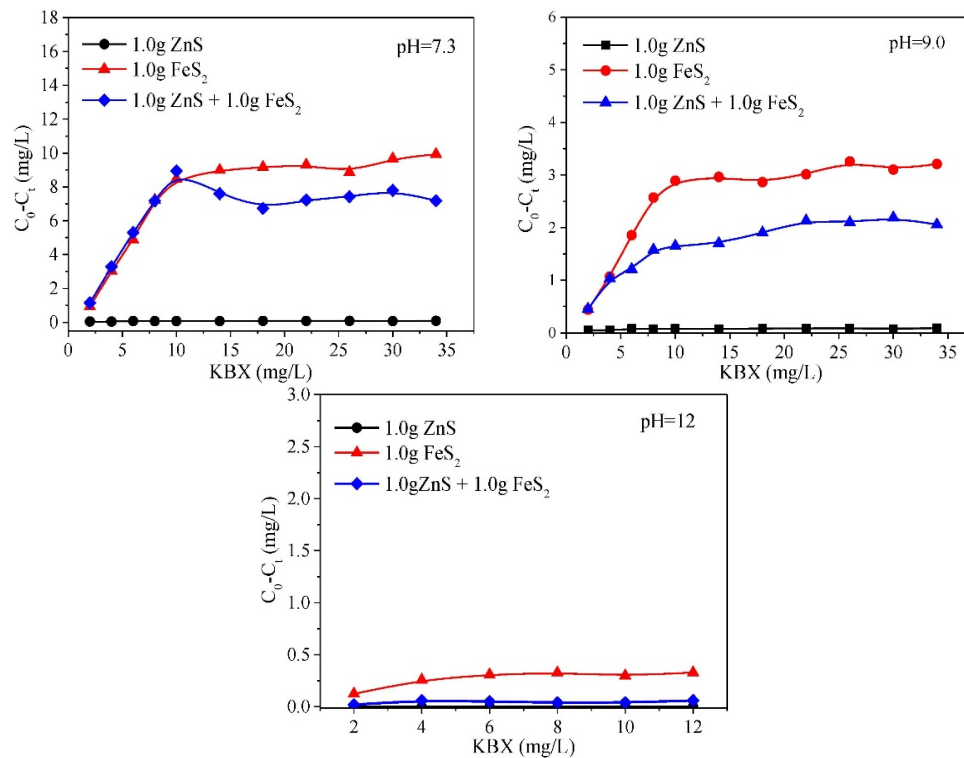


Fig. 5. Adsorption capacity of the KBX collector on the pyrite surface in the presence and absence of sphalerite

suggested that the galvanic interactions between pyrite and sphalerite had a significant influence on the adsorption of xanthate on the pyrite surface, which could decrease the adsorption capacity of the KBX collector on the pyrite surface. However, at the acid and weakly alkaline pH condition, the pyrite has an excellent collectorless and collector-induced floatability, the decreased KBX adsorption on pyrite surface cannot give rise to the decrease in pyrite recovery. This result was consistent with the results from micro-flotation tests. The experimental investigation from Rao and Finch indicated that the adsorption of xanthate on the pyrite surface was significantly decreased from 1.18 to 0.45 monolayers when sphalerite was present in the pulp, and the decrease in the DO level and Eh in pulp was responsible for the decrease in the xanthate adsorption on the pyrite surface (Rao and Finch, 1987).

3.3. Cyclic voltammetry measurements

Cyclic voltammetry scans were conducted to study the effect of galvanic interactions on the electrochemical behavior of pyrite in the presence of the KBX collector. For the purpose of comparison, the voltammetry scans of the pyrite and sphalerite electrodes were also obtained, and each test was conducted at a scanning rate of 10 mV/s and scanning ranges of -0.4 V to 0.8 V; the results are shown in Fig. 6.

For the pyrite electrode (shown in Fig. 6(a)), an obvious oxidation current peak was observed at a scanning potential of 0.2 V, and the oxidation current increased as the potential became more positive. The peak with the initial potential of 0.2 V could be attributed to the oxidation of xanthates to dixanthogen on the pyrite surface, and the oxidation reaction can be expressed as Equation (1).



For Equation (1), the potential can be calculated by the Nernst equation (Equation (2)) (Pecina et al., 2006).

$$E_{X_2/X^-} = E_{X_2/X^-}^\ominus - 0.059 \log [X^-] \quad (2)$$

where E_{X_2/X^-}^\ominus is the standard potential of Equation (1) and $[X^-]$ is the xanthate concentration. In regard to the butyl xanthate collector, the calculated potential value was approximately 0.182 V when 20 mg/L KBX was added, which was basically consistent with the results of the cyclic voltammetry tests. In regard to the sphalerite electrode (shown in Fig. 6(b)), no obvious oxidation current peaks occurred in

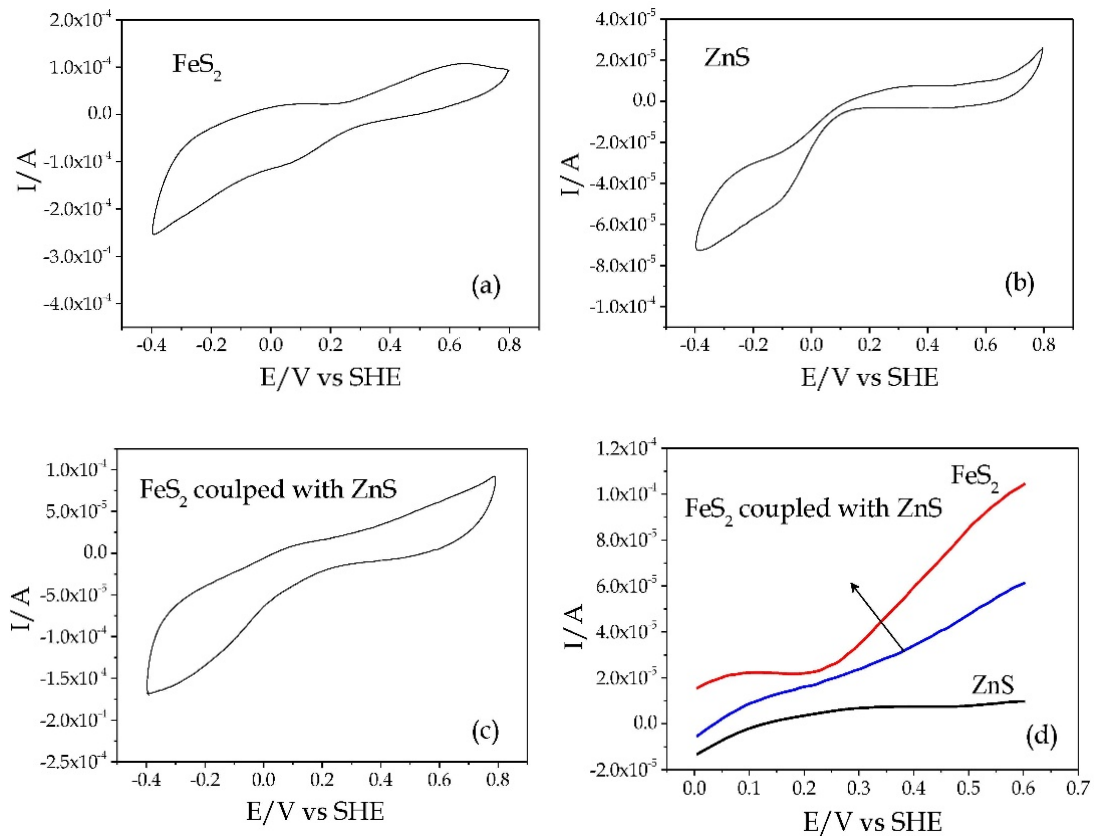
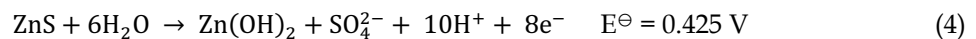


Fig. 6. Cyclic voltammograms of pyrite (a), sphalerite (b), and pyrite coupled with sphalerite (c) and the comparison of current intensities in the range of 0.0 V-0.6 V (d) (pH = 9.18, 20 mg/L KBX)

the scanning potential range of 0.0 V to 0.5 V, which indicated that the unactivated sphalerite reacted poorly with the KBX collector. This result was consistent with the results from the collector adsorption and flotation tests. When the scanning potential exceeded 0.5 V, an anodic current peak was detected on the sphalerite electrode. This peak could be attributed to the oxidation of S²⁻ to S₂O₃²⁻ or SO₄²⁻ on the sphalerite surface and can be expressed by Equation (3).



When pyrite was electrochemically coupled with sphalerite, a relatively weak oxidation current peak was observed at a scanning potential of 0.2 V (shown in Fig. 6(c)). The initial potential of the oxidation peak was uniform with the single pyrite electrode, representing the oxidation of xanthate to dixanthogen on the pyrite surface. However, it was found that the current intensity of the oxidation peak in the scanning potential range of 0.2 to 0.6 V significantly decreased when pyrite was electrochemically coupled with sphalerite. The current intensity comparison of the different electrodes is demonstrated in Fig. 6(d), and the results indicated that the electrochemical coupling of pyrite with sphalerite significantly decreased the oxidation current intensity of xanthate to dixanthogen on the pyrite surface. These results were consistent with the above flotation and collector adsorption tests; thus, the galvanic interaction between pyrite and sphalerite could decrease the adsorption of xanthate on the pyrite surface in acidic and weakly alkaline pH ranges. However, the floatability of pyrite was slightly decreased because pyrite had an excellent collectorless floatability in these acidic and weakly alkaline pH ranges (Aghazadeh et al., 2015; Ozun et al., 2019).

3.4 XPS surface analysis

The results from the flotation tests indicated that the floatability of pyrite clearly improved under strongly alkaline pH conditions (pH > 10) with the presence of sphalerite in pulp, but the collector adsorption tests showed that the adsorption of KBX on the pyrite surface significantly decreased due to the galvanic interaction between pyrite and sphalerite. To investigate the species formed on the pyrite

surface at a strongly alkaline pH and its variation after electrochemical interactions, a surface XPS analysis of pyrite in the presence and absence of sphalerite in the pulp was carried out; the results are shown in Fig. 7.

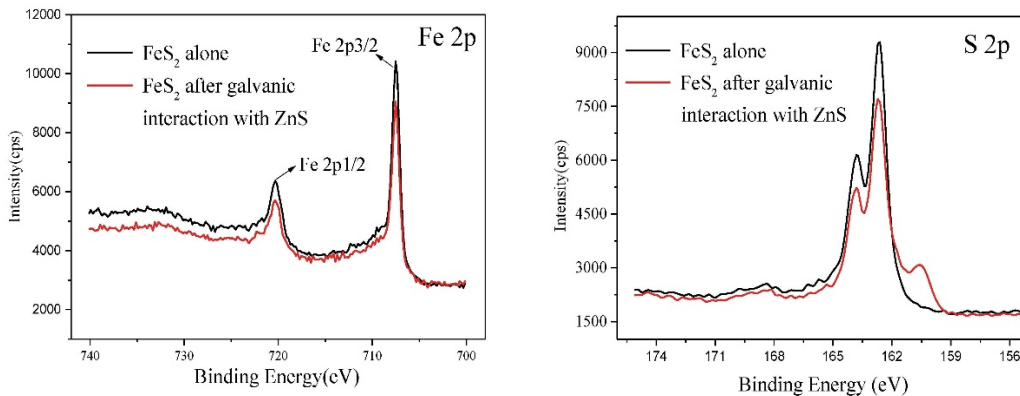


Fig. 7. Fe 2p and S 2p spectra of the pyrite surface in the presence and absence of sphalerite (pH = 12.0)

Fig. 7 shows that the Fe 2p spectrum of pyrite was composed of a strong Fe 2p_{3/2} peak at a binding energy of 708.60 eV and a weak Fe 2p_{1/2} peak at a binding energy of 721.70 eV. The Fe 2p spectrum of pyrite before and after galvanic interaction with sphalerite was almost unchanged, which indicated that the galvanic interaction between pyrite and sphalerite had no influence on the chemical status of the Fe atoms on the pyrite surface. However, the peak shape and position of the S 2p spectrum on the pyrite surface showed an obvious change due to the presence of sphalerite in the pulp, which demonstrated that the chemical status of the S atom on the pyrite surface was altered after the galvanic interaction. To identify the change in the S atom valance states on the pyrite surface, the high-resolution scans of S 2p were carried out, and the fitting peak of S 2p is shown in Fig. 8. In the XPS analysis of S, the S 2p spectra were fitted by using S 2p_{1/2} and S 2p_{3/2} doublets at a fixed 1:2 peak area ratio and a 1.18 eV energy separation (Chen et al., 2014).

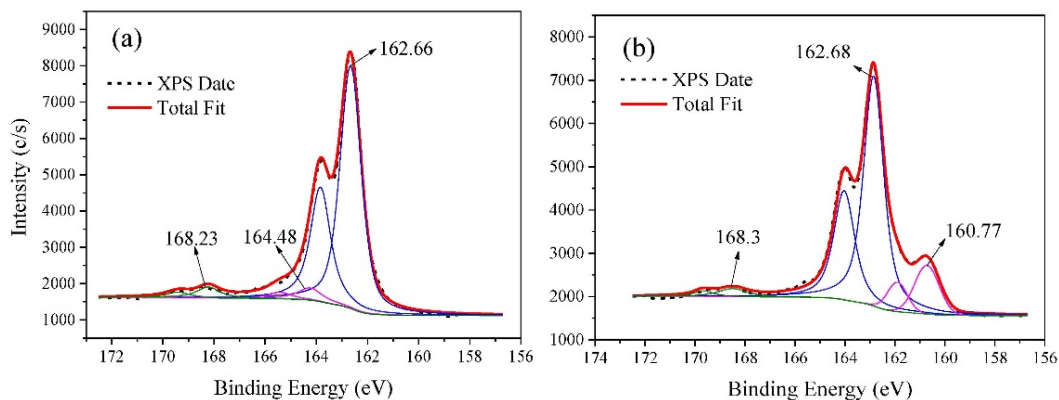
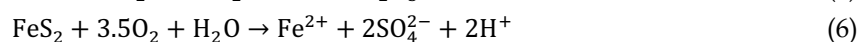


Fig. 8. S 2p fitting spectra of pyrite alone (a) and (b) after galvanic interaction with sphalerite

In Fig. 8(a), the S 2p doublet with S 2p_{3/2} at a binding energy of 162.66 eV was identified as S₂²⁻ from the pyrite surface or bulk, and the S 2p doublet with S 2p_{3/2} at a binding energy of 164.8 eV was attributed to S₂O₃²⁻, which was a hydrophilic oxidation product formed on the pyrite surface. In addition, a relatively weak S 2p doublet at a binding energy of 168.23 eV was detected on the pyrite surface, which represented the SO₄²⁻ oxidation product. The related oxidation reaction can be expressed by Equation (5) and Equation (6).



However, a broad peak with S 2p_{3/2} at a binding energy of 160.77 eV was detected on the pyrite surface in the presence of sphalerite in the pulp (as shown in Fig. 8(b)). The broad peak could be

attributed to S^{2-} , which was a reduction product formed on the pyrite surface due to the reduction of S_2^{2-} to S^{2-} . On the other hand, the S 2p doublet with the S 2p_{3/2} at a binding energy of 164.8 eV, represented the $S_2O_3^{2-}$ oxidation species, disappeared after the galvanic interaction. The XPS results indicated that under strongly alkaline pH conditions, the presence of sphalerite in the pulp alleviated the surface oxidation of pyrite due to the galvanic interaction between pyrite and sphalerite. As a result, the proportion of hydrophilic oxidation products on pyrite decreased, and the floatability of pyrite improved. These results were consistent with the results from the flotation tests and collector adsorption measurements.

4. Conclusions

The effect of the galvanic interaction between pyrite and sphalerite on the floatability and surface characteristics of pyrite was investigated in this work. By comparing the flotation behavior, xanthate adsorption, cyclic voltammetry results, and surface species of pyrite in the absence and presence of sphalerite, the following conclusions were drawn.

(1) Under acidic and weakly alkaline pH conditions ($4.0 < \text{pH} < 9.5$), the floatability of pyrite decreased due to galvanic interactions between pyrite and sphalerite. The decrease in the adsorption capacity of the KBX collector on the pyrite surface was responsible for the decreased floatability.

(2) When pyrite was electrically connected with sphalerite, the oxidation current of xanthates to dixanthogen on the pyrite surface significantly decreased. As a result, the adsorption of xanthates on the pyrite surface decreased.

(3) Under strongly alkaline pH conditions, the galvanic interaction between pyrite and sphalerite inhibited the surface oxidation of pyrite because of the electrons received from the sphalerite surface, and the $S_2O_3^{2-}$ oxidation product on the pyrite surface disappeared after the galvanic interaction. Therefore, the floatability of pyrite improved under strongly alkaline pH conditions after the galvanic interaction.

Acknowledgments

The authors are grateful for the financial support provided by the Yunnan Fundamental Research Project (No. 2019FH001(-091)) and the Opening Research Project from State Key Laboratory of Complex Nonferrous Metal Resources Clean Utilization (No. CNMRCUKF1902).

References

- AGHAZADEH, S., MOUSAVINEZHAD, S. K., GHARABAGHI, M. 2015. *Chemical and colloidal aspects of collectorless flotation behavior of sulfide and non-sulfide minerals*. Adv. Colloid Interface Sci. 225, 203-217.
- AIKAWA, K., ITO, M., SEGAWA, T., JEON, S., PARK, I., TABELIN, C. B., HIROYOSHI, N. 2020. *Depression of lead-activated sphalerite by pyrite via galvanic interactions: Implications to the selective flotation of complex sulfide ores*. Miner. Eng. 152, 106367.
- CHANDRA, A. P., PUSKAR, L., SIMPSON, D. J., GERSON, A. R. 2012. *Copper and xanthate adsorption onto pyrite surfaces: Implications for mineral separation through flotation*. Int. J. Miner. Process. 114-117, 16-26.
- CHEN, X., SEAMAN, D., PENG, Y., BRADSHAW, D. 2014. *Importance of oxidation during regrinding of rougher flotation concentrates with a high content of sulfides*. Miner. Eng. 66-68, 165-172.
- CHOPARD, A., PLANTE, B., BENZAAZOUA, M., BOUZAHZAH, H., MARION, P. 2017. *Geochemical investigation of the galvanic effects during oxidation of pyrite and base-metals sulfides*. Chemosphere. 166, 281-291.
- EJTEMAEI, M., NGUYEN, A. V. 2017. *Characterisation of sphalerite and pyrite surfaces activated by copper sulphate*. Miner. Eng. 100, 223-232.
- HU, Y., WU, M., LIU, R., SUN, W. 2020. *A review on the electrochemistry of galena flotation*. Miner. Eng. 150, 106272.
- HU, Y. H., ZHANG, S. L., QIU, G. Z., MILLER, J. D. 2000. *Surface chemistry of activation of lime-depressed pyrite in flotation*. Trans. Nonferrous Met. Soc. China. 10, 798-803.
- HUANG, P., CAO, M., LIU, Q. 2013. *Selective depression of pyrite with chitosan in Pb-Fe sulfide flotation*. Miner. Eng. 46-47, 45-51.
- LIU, Q., LI, H., ZHOU, L. 2008. *Galvanic interactions between metal sulfide minerals in a flowing system: Implications for mines environmental restoration*. Appl. Geochem. 23, 2316-2323.

- LU, Y. L., TONG, X., XIE, X., YANG, B., HUA, Z. B. 2019. *Effect of particle size on the oxidation and flotation behavior of galena particles*. Physicochem. Probl. Mineral Pro. 55, 208-216.
- MOSLEMI, H., GHARABAGHI, M. 2017. *A review on electrochemical behavior of pyrite in the froth flotation process*. J. Ind. Eng. Chem. 47, 1-18.
- MU, Y., PENG, Y., LAUTEN, R. A. 2016a. *The depression of copper-activated pyrite in flotation by biopolymers with different compositions*. Miner. Eng. 96-97, 113-122.
- MU, Y., PENG, Y., LAUTEN, R. A. 2016b. *The depression of pyrite in selective flotation by different reagent systems – A Literature review*. Miner. Eng. 96-97, 143-156.
- MU, Y., PENG, Y., LAUTEN, R. A. 2018. *The galvanic interaction between chalcopyrite and pyrite in the presence of lignosulfonate-based biopolymers and its effects on flotation performance*. Miner. Eng. 122, 91-98.
- OWUSU, C., BRITO E ABREU, S., SKINNER, W., ADDAI-MENSAH, J., ZANIN, M. 2014. *The influence of pyrite content on the flotation of chalcopyrite/pyrite mixtures*. Miner. Eng. 55, 87-95.
- OWUSU, C., FORNASIERO, D., ADDAI-MENSAH, J., ZANIN, M. 2015. *Influence of pulp aeration on the flotation of chalcopyrite with xanthate in chalcopyrite/pyrite mixtures*. Int. J. Miner. Process. 134, 50-57.
- OZUN, S., VAZIRI HASSAS, B., MILLER, J. D. 2019. *Collectorless flotation of oxidized pyrite*. Colloid Surf. A-Physicochem. Eng. Asp. 561, 349-356.
- PECINA, E. T., URIBE, A., NAVA, F., FINCH, J. A. 2006. *The role of copper and lead in the activation of pyrite in xanthate and non-xanthate systems*. Miner. Eng. 19, 172-179.
- QIN, W.-Q., WANG, X.-J., MA, L.-Y., JIAO, F., LIU, R.-Z., GAO, K. 2015a. *Effects of galvanic interaction between galena and pyrite on their flotation in the presence of butyl xanthate*. T Trans. Nonferrous Met. Soc. China. 25, 3111-3118.
- QIN, W., WANG, X., MA, L., JIAO, F., LIU, R., YANG, C., GAO, K. 2015b. *Electrochemical characteristics and collectorless flotation behavior of galena: With and without the presence of pyrite*. Miner. Eng. 74, 99-104.
- RAO, S. R., FINCH, J. A. 1987. *Electrochemical studies on sulphide minerals with special reference to pyrite-sphalerite. Part I Cyclovoltammetry and pulp potential measurements*. Can. Metall. Q. 163, 521-529.
- REIS, A. S., REIS FILHO, A. M., DEMUNER, L. R., BARROZO, M. A. S. 2019. *Effect of bubble size on the performance flotation of fine particles of a low-grade Brazilian apatite ore*. Powder Technol. 356, 884-891.
- SANTOS, F. E.-D. L., RIVERA-SANTILLÁN, R. E., TALAVERA-ORTEGA, M., BAUTISTA, F. 2016. *Catalytic and galvanic effects of pyrite on ferric leaching of sphalerite*. Hydrometallurgy. 163, 167-175.
- SHEN, P., LIU, D., ZHANG, X., JIA, X., SONG, K., LIU, D. 2019. *Effect of (NH₄)₂SO₄ on eliminating the depression of excess sulfide ions in the sulfidization flotation of malachite*. Miner. Eng. 137, 43-52.
- SOMASUNDARAN, P., WANG, D. 2006. Chapter 4 Mineral-flotation reagent equilibria. Pp. 73-141 in *Developments in Mineral Processing*, vol. 17, ed. D. Wang. Elsevier.
- SONG, S., LOPEZ-VALDIVIESO, A., REYES-BAHENA, J. L., BERMEJO-PEREZ, H. I., TRASS, O. 2000. *Hydrophobic Flocculation of Galena Fines in Aqueous Suspensions*. J. Colloid Interface Sci. 227, 272-281.
- URBANO, G., MELÉNDEZ, A. M., REYES, V. E., VELOZ, M. A., GONZÁLEZ, I. 2007. *Galvanic interactions between galena-sphalerite and their reactivity*. Int. J. Miner. Process. 82, 148-155.
- YANG, B., TONG, X., LAN, Z. Y., CUI, Y. Q., XIE, X. 2018a. *Influence of the Interaction between Sphalerite and Pyrite on the Copper Activation of Sphalerite*. Minerals. 8,
- YANG, B., XIE, X., TONG, X., LAN, Z. Y., CUI, Y. Q. 2018b. *Interaction between sphalerite and pyrite and its effect on surface oxidation of sphalerite*. Physicochem. Probl. Mineral Pro. 54, 311-320.
- ZANIN, M., LAMBERT, H., DU PLESSIS, C. A. 2019. *Lime use and functionality in sulphide mineral flotation: A review*. Miner. Eng. 143, 105922.
- ZENG, Y., LIU, J., RU, S.-S., WEN, S.-M., WANG, Y. 2019. *DFT study the adsorption of ethyl xanthate on the S-site of Cu-activated sphalerite (1 1 0) surface in the presence of water molecule*. Results Phys. 13, 102271.